A CASE STUDY: VELOCITY OF LIQUEFACTION-INDUCED LANDSLIDE IN JONO-OGE TRIGGERED BY 7.5 Mw PALU EARTHQUAKE

Karina A. SUJATMIKO[1] and Koji ICHII[2]

[1]Doctoral Student, Graduate School of Societal Safety Sciences, Kansai University
(7-1 Hakubaicho, Takatsuki, Osaka 569-1098, Japan)
E-mail: k615907@kansai-u.ac.jp (Corresponding Author)
[2]Member of JSCE, Professor, Graduate School of Societal Safety Sciences, Kansai University
(7-1 Hakubaicho, Takatsuki, Osaka 569-1098, Japan)
E-mail: ichiik@kansai-u.ac.jp

On the 28th of September 2018, a 7.5 Mw earthquake in Palu, Indonesia, triggered multiple phenomena events such as liquefaction, landslide, and tsunami. One unique video recorded the landslide in Jono-Oge, located near Palu Valley, captured by a local citizen from his house that was carried along by a debris flow. The video shows that the land moved like water, carrying buildings and trees while some structures remained. The moving camera raises difficulties for the analysis because it operates with various degrees of movement. However, the velocity estimation is possible by applying two types of camera angle analysis using non-moving buildings captured on the video as the point of reference. In this case, a red roof house and steel tower. We identified that the camera moved from east to west and started from elevation 70 m, located 1000 meters from the top of the Jono-Oge landslide at the irrigation canal. At elevation 68 m, the landslide velocity was 5.1 m/s and slowed down to 4 m/s after moving 200 meters to elevation 62 m. This deceleration might correspond to the decrease in slope inclination, from 3% to a gentler slope of only 1%. This result will be informative for the setting of landslide and landslide-induced tsunami simulation.

Key Words : *Palu earthquake, liquefaction, landslide velocity, video content analysis*

1. INTRODUCTION

In the dusk of September 28, 2018, a strike-slip earthquake with magnitude Mw 7.5 occurred in Central Sulawesi, Indonesia. This earthquake leads to multiple phenomena events such as liquefaction, landslide, and tsunami. Creating a catastrophic event that caused 4.340 casualties and near 70.000 damaged buildings, as reported by The National Disaster Management Authority (BNPB) of Indonesia. **Fig. 1** shows the epicenter and shaking intensity estimated by the United States Geologic Survey (USGS). The strong shaking around Palu Valley (MMI 7.0 – 8.0) and massive scale landslides were observed around Palu. After landslides in Palu, Robertson et al. (2019) and Mason et al. (2019) conducted the post-event survey. They concluded that the landslides were due to liquefaction in a wide area. However, the details of the mechanism are not yet clarified. In Palu bay, an underwater landslide also happened and caused a tsunami. Due to a lack of data on the underwater landslide case, researchers are still guessing the landslide characteristic that triggered the tsunami in Palu bay. This study aims to obtain one of the landslide characteristics, specifically the landslide velocity, which cannot be regained from the field survey.

Landslide velocity is an important factor in disaster mitigation; it can be calculated using slope geometry (Souisa et al.,2018), remote sensing (Zhao and Lu, 2018), and real-time video recording (Q. Jiang et al., 2015; Mishra et al., 2015). A real-time video of a landslide may include much information on the slide, such as pre-failure behaviors, failure format, sliding characteristics and velocity, the runout region, post-failure characteristics, and destructiveness (Q. Jiang et al., 2015). To date, there has been no research using video recording focused on liquefaction induced landslide velocity. This study aims to use the available video to calculate landslide velocity because it is

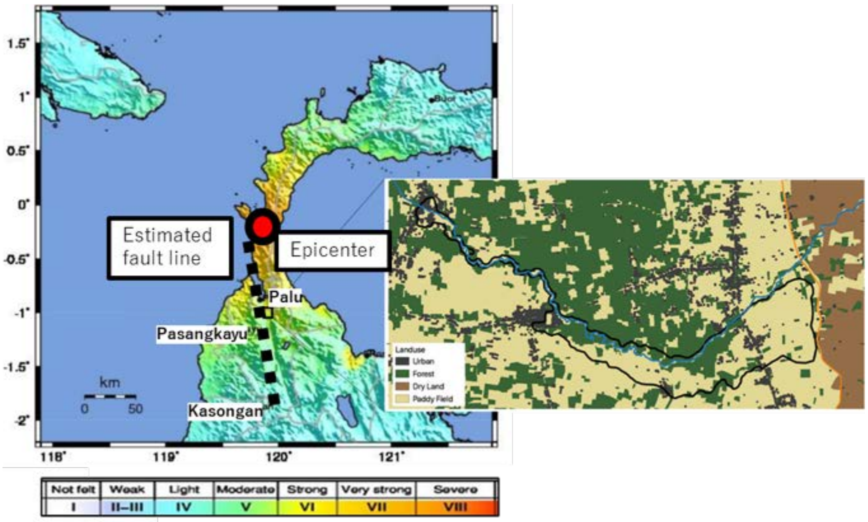

Fig.1 Location of epicenter (red circle), shaking intensity (USGS, 2018) and landslides locations. Insert picture show the Jono-Oge land use map using data from Bradley et.al. (2019).

important to clarify the sliding mechanisms and develop a model with a precise prediction function (Q. Jiang et al., 2015). Furthermore, this velocity infomation can be used as information for landslide-induced tsunami simulation. model with a precise prediction function (Q. Jiang et. al., 2015). Furthermore, this velocity information can be use as information for landslide-induced tsunami simulation.

2. METHODOLOGY

(1) Study area

Based on the field survey carried out by Mason et al. (2019) and Robertson et al. (2019), all the landslides are known to be located along Palu Valley's margins. This V-shaped region is surrounded by mountainous topography and crossed by rivers from south to north. One landslide occurred in the Balaroa area located on the west side of Palu Valley. The other two large landslides occurred on the east side in Petobo and Jono-Oge area. One video posted on social media that recorded the landslide in the Jono-Oge area captured the mud movement similar to waves that indicated the liquefaction phenomena.

This large-scale liquefaction induced landslides had been reported in the world. For example, in the 1964 Niigata earthquake, the lateral flow lasted for several minutes after the end of ground motion shaking (Kawakami and Asada, 1966). The ground lithology in Niigata was found to be stratified with a silty sub-layer sandwiched between the loose sandy layer (Kishida, 1966). However, the Jono-Oge landslide's fatality is far more extensive than the reported Niigata case; therefore, a more detailed study on the Jono-Oge landslide is necessary. Based on the Jono-Oge land-use map (**Fig.1**), the majority of this area is used for paddy field and gained water from the irrigation canal. The fields survey (Mason et.al., 2019; Robertson et.al, 2019) revealed that the starting point of all landslides in the east side, including Jono-Oge, was bounded by an irrigation canal. Research suspected irrigation on this paddy field has raised the water table and could create a liquified layer. The landslide appears to have initiated when the elevation transitioned from 80 to 70 m, as the slope getting gentler from around 4% to 1% as shown in **Fig.2**.

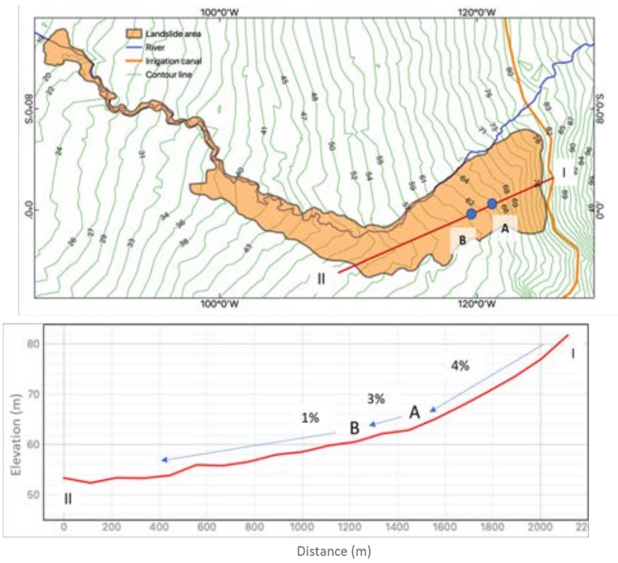

Fig.2 The elevation contour and slope of Jono-Oge landslide.

(2) Video recording during Jono-Oge landslide

No instrument recorded the shaking at the site. However, there was a survivor who recorded this landslide. The video snapshots (**Fig. 3**) were used as material for video content analysis. This research will apply video content analysis (VCA) to determine the velocity of the recorded landslide. The video used in this research was captured by survivors during the landslide and opened on social media. In his social media page, he shared about the chronology. He climbed to the rooftop of his house when he felt the strong ground motion, then the ground starts to move, and he recorded the situation using his smartphone. This video's uniqueness is that it was taken from the house that was brought along by a debris flow. The video shows the land movement flowed like water that carried along with buildings and trees while some remain on the ground.

Fig.3 Image sequence in the video.

VCA was analyzing through image sequence using ffmpeg program (www.ffmpeg.org) converted into one image per second. With the video duration 2 minutes and 5 seconds, there are 125 images produced. We chose the necessary sequences: the beginning of the video to identify the recording location and scenes of unmoved structures to analyze camera angle and position. The video was recorded by mobile phone made the video has some problems in the quality aspect and motion. This video categorizes as a low-quality resolution due to video compression that caused block artifacts. The camera vibration caused a blurry effect to the video sequence. Unlike the fixed camera, the moving camera operates with various degrees of movement and autonomy. In the simple case of a fixed camera, the only changes between consecutive frames are caused by moving objects; therefore, it is easier to use auto-tracking motion program. The difficulties in using the moving camera arise when detecting moving object due to changes of possible camera's depth and complex movements (Yazdi and Bouwmans, 2018). Therefore, we eliminate using auto-tracking motion program to obtain the landslide velocity. Instead, we use information from the past survey report, satellite imagery, DEM data, and apply basic rules of geometrical optics and perspective vision with Google Earth and QGIS tools to determine the location, pathway, and velocity of the recorded landslide.

(3) Methodology of video content analysis

The velocity was calculated using a simple formula as described in equation (1). To be able to use the formula, two essential components are required, namely where the start and end location (l_0 and l_1) are and how long (t_0 and t_1) it takes when recording the start and end locations. We can get this information through video content analysis. Stages of analysis are divided into three parts, namely initial location identification, camera movement path estimation, and camera angle analysis.

$$v = \frac{L}{T} = \frac{l_1 - l_0}{t_1 - t_0} \tag{1}$$

The first step is to identify the initial location where the recording started. Note, in practice, we conducted the initial location identification after the estimation of the camera movement direction, as explained later. The second step is to estimate the path and direction of the camera movement. This step was necessary because this video was recorded from the top of the house, which was carried away by a landslide. Based on the survey (Mason et al., (2019); Robertson et al. (2019)) and satellite imagery, it is known that the recorded landslide occurred in the Jono-Oge area and moved from east to west.

The third step is camera angle analysis to determine the exact location of the camera when capturing an object. In this step, the reference object is needed to determine the location of the camera. For this purpose, we used two structures in the recorded video shown in Fig. 3: the red-roofed house and steel tower. Using the digital imagery from the digital globe taken after the disaster on September 28, 2018 it is found there is one red-roofed house in the middle of Jono-Oge Landslide with the coordinate -0.98579, 119.91965. Comparing with the satellite image taken before the disaster, confirm that the red-roofed house has the same coordinate and indicate it was not moving during the Jono-Oge landslide. This result also validates with the survey conducted by Mason et .al (2019) and Robertson et al. (2019). They found the red-roofed in Jono-Oge, and even though the mud flowing through the building, it stays in that original position. The steel tower, although not found in the post-disaster satellite image, was used as a reference object. This is possible because the steel tower is recorded clearly and close enough to the camer in the shoot time of the scenes used in the analysis.

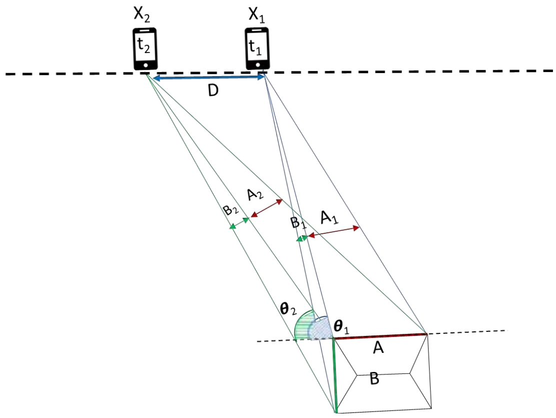

Fig.4. Method using ratio of object in the image sequence to calculate camera angle.

The camera angle analysis for the red-roofed house was done as follows using the ratio of some lengths in images of a reference object. When the camera not straightly facing an object, the angle becomes smaller and will appear smaller. Thus, as shown **Fig. 4**, the angle of recording can be calculated from the ratio of the sizes of 2 walls in different directions.

$$\theta_i = \arctan\left(\frac{A_{i/A}}{B_i/B}\right) \qquad (2)$$

The camera angle analysis mentioned above couldn't be applied for steel tower since there were no clear walls. Instead, the angle calculated using two continuous image sequence was used. If the time difference between the two images is so short and we can assume the camera direction is not moving, the pixel difference (Dp) of the object in the image relates to the difference in the angle to the object (θ) as shown in **Fig. 5**.

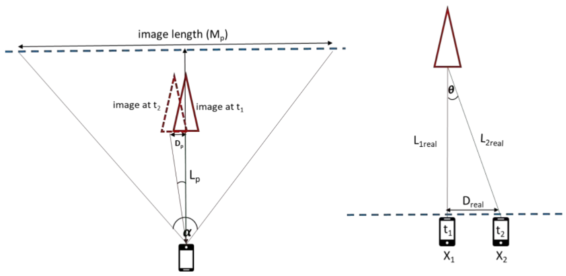

Fig.5 The angle analysis using pixel difference between image sequence to calculate angle.

Thus, the ratio of the pixel difference and the image length (Dp/Mp) relate to the ratio of the difference in the angle to the object (θ) and angle of view of the camera (α), as shown in equation (2). Then, if the distance to the object is known (L_{real}), the movement of the camera (D_{real}) can be obtained from equation (3a) and (3b). Pixel difference (Dp) was obtained by placing a mark on the same object in the continuous images. Because the camera moves, even the camera direction is the same, there will be a change in the position of the object in the following images. The change of the object in the image is measured by determining a point on the object in images.

$$\frac{\theta}{\alpha} = \frac{D_p}{M_p} \qquad (3a)$$

$$D_{real} = L_{real} \,.\, \tan\theta \qquad (3b)$$

3. RESULT

(1) Identification of landslide movement direction

Along 125 seconds of the video, there are two structure can be identified, a house with a red roof (recorded during 20 – 35 second) and steel tower (recorded during 65 – 102 second) as shown in **Fig.6**. From the 103 seconds until the end of the video recording only a tree was recorded and no other buildings could be identified. From the post-disaster survey report by Mason et.al. (2019), they found the ruins of a church in coordinate -0.98942, 119.91007. This church was originally located at coordinates -0.98508, 119.919244 and only 50 meters away from the red-roofed house as shown in **Fig. 6.**

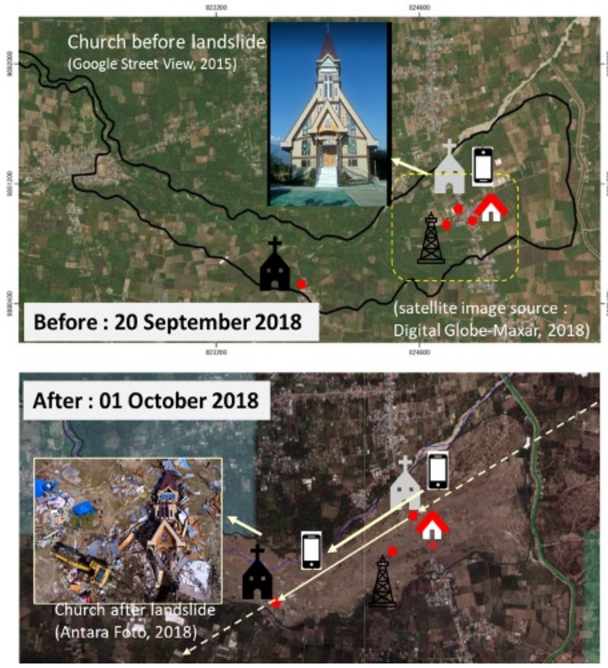

Fig.6 Identified building from the video plotted in the satellite image before and after the landslide happened. Possible landslide pathway connected by the church (GPID Patmos Jono Oge) before and after landslide happened.

Landslide pathway determined by drawing a solid line from the original position of the church before the disaster and the church position after the disaster, as shown in **Fig. 6.** The location of the red-roofed house is in the east direction of the church, so it needs to add a line that illustrates the possibility of extending the landslide path as the dotted line. We assume all the houses near here moved parallel to the estimated pathway.

(2) Identify initial location of the video

The initial location of recording video is unknown, however there are some information that 1) the house already moving before the video starts recording, 2) there was no others house in the right and left, and 3) in the initial recording the camera video capturing the area surrounded by trees and paddy field. From the video analysis and satellite image, there is a house that almost on the dotted line, which is the possible landslide pathway obtained from the church location. The situation around the house also similar to the landscape capture on the video. Thus, we identify the house as the possible location of the initial point of the video recording with the coordinate at 0.98450 S, 119.92089 E and we assume the position of video recording moved parallel to the church landslide pathway as we can see in **Fig 7.**

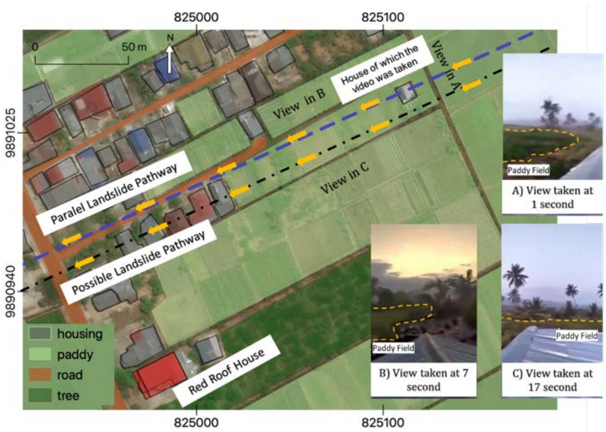

Fig.7 Landscape and situation captured in the beginning of video along the first 17 seconds.

(3) Image angle analysis using ratio of length: red-roofed house case

The reference object in the analysis is the rooftop of the red-roofed house. After careful selection, images used in the analysis are at t = 27s and t = 30s as shown in **Fig. 8.** The angle degree calculated by ratio method using **Equation 2**.

Table 1 Parameters and distance calculation by ratio method using red-roofed house image sequence.

Time (s)	27	30
A (pixel)	83	57
B (pixel)	22	28.7
Ratio A	0.8	0.7
Ratio B	0.2	0.3
Angle (degree)	75.15	63.27
Distance (meter)	80.9	86.5

Fig.8 Images for the angle analysis of red roofed house.

The estimated angles of these images are summarized in **Table 1**. Then, the possible camera locations were identified in line with the possible land-slide pathway as shown in **Fig. 9**. From this plot, we obtain the length between point X_1 to X_2 is 15.3 m. Then, using the equation (1), $L \approx 15.3$ m , $t1 - t0 = 3$ s, and velocity (v) ≈ 5.1 m/s.

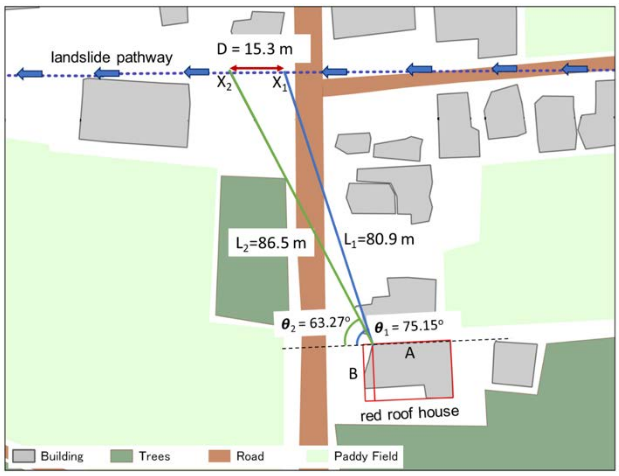

Fig.9 Plot of camera position on the possible landslide pathway.

(4) Image angle analysis using ratio of length: steel tower case

Another image used to estimate the velocity is the sequence showing the steel tower. However, the tower has no clear two faces of the wall to adopt the method used in the red-roofed house. Instead, we focused on the scenes at t = 70 seconds and 71 seconds. In these two pictures (**Fig. 10**) the background is the same cloud shape as marked by the blue dashed line in the two left-sided pictures.

Table 2 Parameters and velocity for angle analysis using steel tower image sequence.

Image length (pixel)	198
Field of view (degree)	79.8
Average pixel difference	4
Min. distance (meter)	91.32
Velocity (m/s)	3.1

The angle of view can be found from the lens specification using in the camera. On the website (www.demitri.asia) there is an article posted the comment from the person capturing the video. He said that he recorded this video using OPPO A57 smartphone device. The lens specification of this A57 camera using sensor model Sony Exmor RS with the aperture f/2.2 and angle of view 79.8^o (www.devicespecifications.com).

Pixel difference (Dp) of the steel tower images obtained by overlaying the shoot at 71 seconds on the top of the shoot at 70 seconds as shown in Fig. 11. The red dashed line showing the edge line of steel tower at t=70s and the yellow dashed line for t=71s showed there is a clear distance between these two pictures. We mark several points at the object edge where every point owns pixel location coordinate. It is found that the maximum pixel difference is 4.75 and the average pixel difference is 4.

Fig.10 Overlay image of steel tower taken at 70 and 71 seconds.

We do not know where the exact location when the video was taken at t=70s. Thus, we calculate the minimum value of the landslide velocity by assuming the first picture taken in the shortest distance between the steel tower and the landslide pathway, which is the perpendicular line to the possible landslide pathway will be given. In this case, using the satellite image, it is found the length (L_1) is 91.32 m. Then, using the information on **Table 2**, it can be found that the angle difference θ = (4.0 pixel/198 pixel) (79.8^o) = 1.91^o, camera movement D = (91.32 m) (tan 1.91^o) = 3.1 m. Since time difference $t_1 - t_0$ = 1 second, the velocity (v) is $\approx$ 3.1 m/s. Note this is a minimum value of the velocity since the minimum value of the distance is assumed.

(5) Verify velocity using pixel difference of the red-roofed house

In the previous section, the landslide velocity estimated from the red-roofed house is 5.1 m/s. We tried to verify the estimated value using the method applied to the steel tower. After scrutinized the image sequence cut by one second there was no satisfying image that can be used to measure the pixel difference. So, the video divided into tighter time, per 0.5 seconds. We found the image recorded at t_1=32.5s and t_2=34s was suitable to apply this method.

Table 3 Parameters and velocity for pixel difference analysis using red-roofed house image sequence.

Point	Pixel	Angle (θ)	Velocity (m/s)
A_1 to A_2	39.2	4.81	5.1
B_1 to B_2	38.4	4.68	5.0
C_1 to C_2	40	4.87	5.2

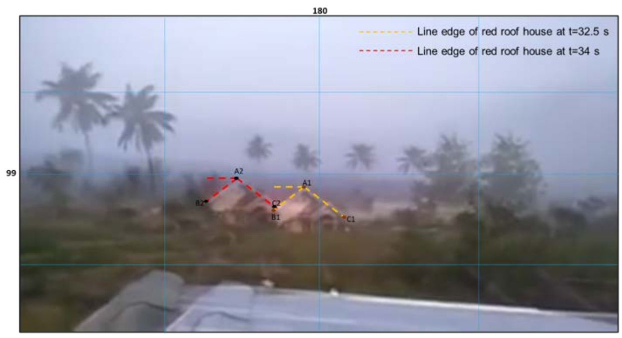

Fig.11 Overlay image of red-roofed house taken at 32.5 and 34 seconds.

Overlaying image at 32.5s with 34s, as in **Fig. 11**, show that the red-roofed house moved to the left, this is as same as the case of the steel tower. Note, the picture changes horizontally and vertically, but we only pay attention to pixels changes in the horizontal direction. The pixel calculation and picture parameters can be seen in **Table 3**. Here, the camera location at t=32.5 s is estimated from the results of the ratio method. In detail, the horizontal distance = 5.1 m/s x 2.5 second = 12.75 meter. Using satellite imagery, the estimated distance of the camera position to the red-roofed house is 92.2 m. The angle of view is 79.8°. Also, the image position changed from portrait to landscape. Thus, the image length is 360 pixels, which is 1.82 times greater than the image length portrait (198 pixels). From the three-point shown in **Fig.11** (A, B, and C), we found the velocity range from 5.0 – 5.2 m/s and the average velocity is 5.1 m/s. In the first method, using image ratio, we found velocity is also 5.1 m/s. Therefore, there is no difference result between these two methods. Thus, we could say that our first estimation of the landslide velocity is quite reliable.

(6) Verify velocity using the possible location of steel tower

This estimated landslide average velocity (5.1 m/s) was then used to calculate the travel distance from red-roofed to steel tower. It possible that the velocity is decreasing along the way, the average velocity 5.1 m/s, gained from the two previous calculation methods using the red-roofed house as an object reference, is used to find the maximum distance from red-roofed last image to the steel tower first image position. The time duration in the video from capturing red roof last image and steel tower first image is 40 seconds. Thus, the horizontal distance (D) = 5.1 m/s x t 40s = 204 m. Then the camera position should be in B2 (**Fig. 12**) and the vertical distance from steel tower to possible landslide pathway around 118.5 m. With this new distance, the estimated landslide velocity changes to 4.0 m/s. It is faster from the previous calculation (v = 3.1 m/s). There is 0.9 m/s or 26% difference with the previous velocity calculation. However, in the previous calculation, we assume the steel tower picture taken perpendicular to the landslide pathway, and the value was given as the minimum value. The slope at the position B2 is gentler than the slope at the position A1 and A2. Thus, the landslide velocity may be decreasing after t=32.5 s.

(7) Discussion of all the possible velocities

Applied various method using red roofed house and steel tower as the reference object, the estimated velocity varied from 3.1 m/s – 5.1 m/s as summarized in **Table 4** and **Fig. 12**.

Table 4 Summary of the estimated velocities.

Location	Method	Velocity (m/s)
A_1	Ratio of red roof house.	5.1
A_2	Pixel difference of red roof house.	5.1
B_1	Pixel difference of steel tower at minimun distance.	3.1 (Minimum)
B_2	Pixel difference of steel tower at the calculated distance.	4.0

From this result it is known that the velocity become slower with from point A2 to B2. The velocity range is -0.9 m/s to -2 m/s. As we can see in **Fig. 2**,

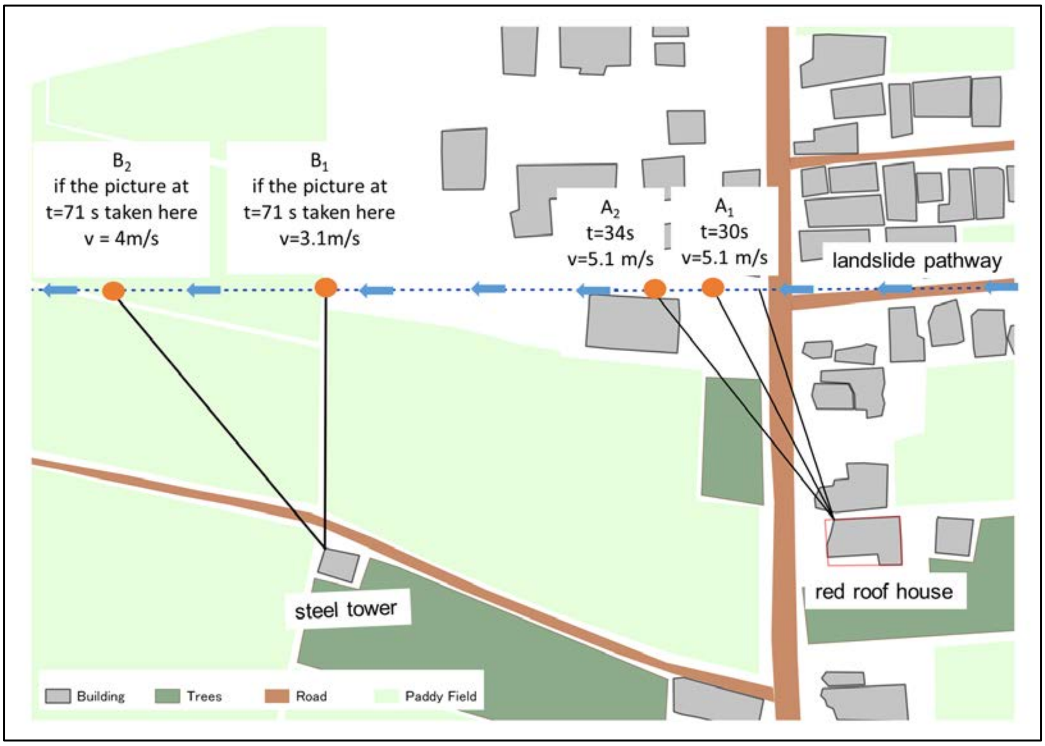

Fig.12 Map plot of velocity variation at the different camera position.

using the map it is known the red roofed house located 1600 m from the top of irrigation location, where the landslide started. The elevation changes from 80 m to 66 m, so the slope is around 3%. While after 1600 m to 1000 m the elevation changes from 66 m to 58 m, makes the slope only around 1 %. Landslide acceleration is related to the slope, therefore, it is possible that one of the reasons maybe the gentler slope that makes velocity slowing down. Thus, our estimation of the landslide velocity is quite consistent and reliable.

4. CONCLUSION

In this research, we applied video content analysis (VCA) to estimate the Jono-Oge landslide's velocity triggered by the 2018 Palu Earthquake. The difficulty of the analysis was that the video was taken from the house that moved along in a debris flow. The significant conclusions obtained in the study are as follows :

(1) Velocity estimation using video images from a moving camera is possible by applying two types of camera angle analyses, the ratio method and pixel differences method.

(2) The possible landslide and video pathway were successfully identified using the video scenes and church building near the recording video location.

(3) The estimated landslide velocity is around 5.1m/s, along 1600 m to 1700 m from the east's irrigation canal. This velocity gained from the analysis using unmove structure images.

(4) The estimated landslide velocity was slowing down to 4 m/s after the camera moves around 200 meters from the red roof house (1900 m the east's irrigation canal). This result corresponding to the slope inclination from 3% in the beginning then decreasing into the gentler slope by 1%.

For further research, this velocity result can be used as information for the setting parameter of landslide simulation or landslide-induced tsunami simulation in Palu. Also, complete information is more suited to determine proper countermeasures in the liquified area.

REFERENCES

1) BNPB (2019). https://bnpb.go.id/publikasi/infografis/infografis- gempabumi-m74-tsunami-sulawesi-tengah.html (accessed 3 February 2020).
2) Bradley, K., Mallick, R., Andikagumi, H, Hubbard, J, Meilianda, E, Switzer, A, Du, N, Brocard, G, Alfian, D, Benazir, B, Feng G, Yun, S-H, Majewski J, Wei S, Hill EM (2019) Earthquake-triggered 2018 Palu Valley landslides enabled by wet rice cultivation. *Nat Geosci* 12:935–939. https://doi.org/10.1038/s41561-019-0444-1
3) Cipta, A., Robiana, R., Griffin, J. D., Horspool, N., Hidayati, S., and Cummins, P. R. (2016). A probabilistic seismic hazard assessment for Sulawesi, Indonesia. *Geol. Soc. Lond. Spec. Publ.* 441, 133–152. doi: 10.1144/sp441.6
4) Jiang, Q., Chan, D., Xiong, J., Cui, Y., Dong, J., Li, D. (2015). Back analysis of a debris landslide based on a real-time video recording: sliding process and post-slide investigation. *Bull. Eng. Geol. Environ.* Doi: 10.1007/s10064-015-0831-9.
5) Mason, B., Gallant, A.P., Hutabarat, D., Montgomery, J., Reed, N., Wartman, J., Irsyam, M., Prakoso, W., Djawardi, D., Hanifa, R. (2019). GEER - Geotechnical Reconnaissance: The 28 September 2018 M 7.5 Palu-Donggala, Indonesia. Technical Report version 1.0.
6) Mehran Yazdi, Thierry Bouwmans. New Trends on Moving Object Detection in Video Images Captured by a moving Camera: A Survey. *Computer Science Review*, Elsevier, 2018. ffhal-01724322f.
7) Pedrotti, L. S. (2017). Basic geometrical optics. In C. Roy-choud-huri (Ed.), *Fundamentals of Photon*ics (pp. 73–116). Bellingham, WA: Society of Photo-Optical Instrumentation Engineers.
8) Robertson, I., Esteban, M., Stolle, J., Takabatake, T., Mulchandani, H., Kijewski-Correa, T., Prevatt, D., Roueche, D., Mosalam, K. (2019). StEER - Palu Earthquake and Tsunami, Suwalesi, Indonesia: Field Assessment Team 1 (FAT-1) Early Access Reconnaissance Report. Structural Extreme Events Reconnaissance, DesignSafe-CI , doi:10.17603/DS2JD7T.
9) Souisa, M., Hendrajaya, L., Handayani, G. (2018). Study on Estimates of Travel Distance, Velocity and Potential Volume of Amahusu Sliding Plane using Energy Conservation Approach in Conjunction with Geoelectric Survey. *J. Math. Fund. Sci*., Vol. 50, No. 2, 2018, 166-181
10) Thein, P. S., Pramumijoyo, S., Brotopuspito, K. S., Kiyono, J., Wilopo, W., Furukawa, A., et al. (2014). Estimation of seismic ground motion and shaking parameters based on microtremor measurements at Palu City, Central Sulawesi Province, Indonesia. *Int. J. Geol. Environ. Eng*. 8, 308–319.
11) USGS (2018) https://www.usgs.gov/news/magnitude-75-earthquake-near-palu-indonesia. (Accessed 3 February 2020)
12) Watkinson, I.A., Hall, R. (2019). Impact of communal irrigation on the 2018 Palu earthquake-triggered landslides. *Nat Geosci* 12:940–945. https://doi.org/10.1038/s41561-019-0448-x.
13) Zhao, C., Lu, Z. (2018). Remote Sensing of Landslides—A Review. *Remote Sens.*10, 279; doi:10.3390/rs10020279
14) http://www.demitri.asia/2018/10/ini-dia-sang-perekam-video-likuifaksi.html (accessed on 3 February 2020)
15) https://www.devicespecifications.com/en/model/2f4f3fd2 (accessed on 3 February 2020)
16) https://godreports.com/2018/10/indonesia-church-carried-a-mile-swallowed-up-after-ground-liquified/ (accessed on 20 February 2020)